GEDI: A New LiDAR Altimetry to Obtain the Water Levels of More Lakes on the Tibetan Plateau

Juan Wu, Chang-Qing Ke, Yu Cai, Vahid Nourani, Jun Chen, and Zheng Duan

***Abstract*—Remote sensing is an effective means for lake water level monitoring on the Tibetan Plateau (TP). The purpose of this study is to estimate water levels of lakes on the TP using the Global Ecosystem Dynamics Investigation (GEDI) and Cloud and Land Elevation Satellite-2 (ICESat-2), evaluate the performance of ICESat-2 and GEDI in estimating water levels, and analyze the differences of water level obtained by the two altimeters. The results showed that the average coefficient of determination (R^2) values between the estimated water levels (GEDI and ICESat-2) and the datasets (DAHITI and Hydroweb) were greater than 0.80, respectively. The water level of DAHITI and Hydroweb are mainly from radar nadir altimeters. The average root mean square error (RMSE) between GEDI and DAHITI was 0.54 m, between GEDI and Hydroweb was 0.38 m for Qinghai Lake. The average RMSE of Qinghai Lake between ICESat-2 and DAHITI was 0.50 m, and between ICESat-2 and Hydroweb was 0.28 m. The comparison results showed that the accuracy of GEDI seems to be slightly lower than that of ICESate-2. The main impact indicators of the difference between the GEDI and ICESat-2 in lake level estimations were the viewing angles (VAs), solar elevation, air temperature, and wind. From 2019 to 2021, GEDI covered 770 more lakes than ICESat-2, and the lake level fluctuation mainly occurred in the Inner Plateau and Yangtze basins. The GEDI can effectively estimate lake levels, which provides more water levels for lakes and lays a foundation for future research on the TP.**

***Index Terms*—GEDI, ICESat-2, lake level, Tibetan Plateau.**

I. Introduction

LAKES are an important part of Earth's freshwater storage [1], [2]. Monitoring changes in lake levels reflects human use of these water resources and indicates climate change [3], [4], [5]. Monitoring lake levels is necessary and important work for water resource utilization management in the national ecosystem sector as well as for humans to address global climate change [6], [7]. Traditional field survey data are limited and scarce due to high construction and maintenance costs and are often considered to be sensitive information [8], [9]. Remote sensing technology provides the opportunity for large-scale lake level measurements to be obtained, and satellite altimetry technology is one of the reliable means to monitor lake level changes [3], [8], [10], [11].

With the development of remote sensing technology and the increasing demand for data, an increasing number of altimeter missions have been launched, and more than ten radar altimeters have been launched (including Geosat, European Remote Sensing Satellite ERS-1/2, Topex/Poseidon, Envisat, Jason1/2/3, Cryosat-2, HaiYang-2, Saral/Altika, and Sentinel 3A/B). Radar altimeters have the capability of all-weather observation and cloud penetration, and existing radar altimeters can already realize the monitoring of long time series [12], [13], [14], [15]. Early radar altimeters, such as Topex/Poseidon, ERS-1/2, Envisat, and Jason-1/2, have achieved long-term lake level monitoring from 1992 to 2019 [12]. The use of multiple radar altimeters improves the temporal resolution of the observation data and provides fundamental data for seasonal lakes studies on the Tibetan Plateau (TP) [13], [14]. Although radar altimeters have been widely used in water monitoring, their large footprints make their accuracy lower than lidar altimeter [16]. Moreover, the orbit drifts enable lidar altimeters to collect measurements over a larger area of the earth's surface than radar altimeters [17]. Only three laser altimeters have been launched, including the Ice, Cloud, and Land Elevation Satellite (ICESat), the Ice, Cloud and Land Elevation Satellite-2 (ICESat-2), and the Global Ecosystem Dynamics Investigation (GEDI). While only ICESat-2 and GEDI are on mission now. The ICESat is the earliest laser altimeter and has been in operation for approximately 7 years, from January 2003 to February 2010 [18]. The ICESat-2 and GEDI were launched in September 2018 and December 2018, respectively. The ICESat and ICESat-2 have been widely used in surface monitoring, including lake level change [10], [19], polar sea ice thickness [20], [21], forest tree height [22], [23], and glacial mass balance [24]. The Satellite lidar measurements have smaller footprints and higher sampling density than radar altimeters, which provides a higher accuracy of lidar measurements. However, the observation error caused by the attenuation and scattering of lidar signal caused by clouds cannot be avoided [25], [26], [27]. The repeat-track mode of

Manuscript received 7 November 2022; revised 7 January 2023 and 16 March 2023; accepted 17 April 2023. Date of publication 19 April 2023; date of current version 2 May 2023. This work was supported in part by the National Natural Science Foundation of China under Grant 42011530120, Grant 41830105 and Grant 41901129, and in part by The Swedish Foundation for International Cooperation in Research and Higher Education under Grant CH2019-8250. *(Corresponding author: Chang-Qing Ke.)*

Juan Wu, Chang-Qing Ke, and Yu Cai are with the School of Geography and Ocean Science, Nanjing University, Nanjing 210023, China (e-mail: wujuan_1706@163.com; kecq@nju.edu.cn; caiyu@nju.edu.cn).

Vahid Nourani is with the Center of Excellence in Hydroinformatics and Faculty of Civil Engineering, University of Tabriz, Tabriz 5166616471, Iran, and also with the Faulty of Civil and Environmental Engineering, Near East University, 99138 Near East Boulevard, Turkey (e-mail: nourani@tabrizu.ac.ir).

Jun Chen is with the Department of Environmental and Energy Engineering, Anhui Jianzhu University, Hefei 230000, China (e-mail: gischen@126.com).

Zheng Duan is with the Department of Physical Geography and Ecosystem Science, Lund University, 223 62 Lund, Sweden (e-mail: zheng.duan@nateko.lu.se).

This article has supplementary downloadable material available at https://doi.org/10.1109/JSTARS.2023.3268558, provided by the authors.

Digital Object Identifier 10.1109/JSTARS.2023.3268558

ICESat-2 and slight adjustment over the land area to make more land surface observed (especially vegetation), but the track spacing in mid-latitude area will become larger than high latitude [28]. The ICESat, ICESat-2, and GEDI have footprints of ∼70 m, 17 m, and 25 m, respectively. In addition, the ICESat and ICESat-2 provide a higher precision in lake level monitoring than radar altimeters and enable monitoring of a much larger number of lakes [10], [12], [19], [29], [31], [32]. Also, if ICESat-2 has more ground tracks, the repeat period would be longer than most radar altimeters. For example, ICESat-2 enables retrieval of annual, seasonal, monthly, and ten-day coverage patterns for 21 pan-Arctic lakes [33]. While the GEDI aims to advance the understanding of carbon and water cycle processes, biodiversity, and habitats, high-precision elevation measurements are also of great value for forest management, glaciers, surface water monitoring, and more accurate DEM generation [33]. Although a few studies have shown that the GEDI performs well in surface water monitoring [35], [36], [37], there remains a lack of further confirmation of the feasibility of the GEDI water level inversion with a large number of samples.

Depending on the state of the data collected by the altimeter, the outside environment, and the size of the lake, the accuracy of the lake level estimation may vary from centimeters to decimeters [37], [38]. The viability of the echoed LiDAR data can be affected by atmospheric factors, such as cloud height, cloud thickness, and cloud optical depth [26]. Different footprint sampling and coverage states also affect the accuracy of lake level extraction [39], [40]. Therefore, it is important to analyze the impact indicators of lake level estimation to improve the accuracy of lake level estimation, which serves as a reference for the comprehensive use of multisource altimetry data.

As an important water reservoir resource and climate indicator, lake level monitoring on the TP is important for the implementation of sustainable development strategies in the ecosystem sector [41], [42]. The TP covers a vast territory and has complex terrain, making field operations difficult, and few lake water levels have been observed in the field [16]. The development of remote sensing technology has facilitated research on the change in lake level on the TP. However, due to the large footprint of radar data (for example, the Topex/Poseidon has a footprint of approximately 2.2 km), in the early stage, levels from only 20 lakes on the TP could be obtained [12]. With the ICESat and ICESat-2 being used to monitor water levels, the ICESat can obtain 4 years of water level data for 100 lakes from 2003 to 2009 [32]. For the lakes on the TP, the number of observed lakes was relatively small, and at least half of the lakes have not yet been observed. The combination of multisource altimetry data can improve the spatial and temporal resolution, and it is an inevitable trend to combine multisource altimetry data to obtain longer lake levels and more lake observations [3], [13], [43], [44]. Since the publication of the latest GEDI lidar altimeter data, the GEDI has been applied to estimate lake levels on a small scale [17], [35], [36]. Currently, the research on lake levels retrieved by using GEDI is mainly focused on the Great Lakes and a small part of the lakes in Switzerland [17], [35], [36]. There are few research using GEDI to retrieve the lake level on the TP, with only one study focused on the water levels of Qinghai Lake [45]. TP is the largest group of plateau lakes on Earth, how does the lake level retrieved by GEDI perform on the TP? Could the combination of the latest laser altimeter provide a new prospect for lake level monitoring on the TP? These are questions worth answering.

Therefore, this study aimed to combine the GEDI and ICESat-2 to obtain the water levels of more lakes. The GEDI and ICESat-2 were used to estimate the lake levels on the TP from June 2019 to June 2021. We compared the performance of the GEDI and ICESat-2 in the estimation of lake levels on the TP and discussed the impact of meteorological factors and altimeter parameters on the water level estimation results. Therefore, we combined the results obtained from the GEDI and ICESat-2 to provide lake level changes and a lake level dataset on the TP from 2019 to 2021.

II. Materials and Methods

A. Study Area

The TP is located at 25°35'N-40°15'N, 67°33'E-104°51'E (see Fig. 1), and with an average elevation of approximately 4000 m a.s.l., it is referred to as "the Third Pole of the world" [41]. There are approximately 2000 lakes of various sizes on the TP, which is the largest group of plateau lakes on Earth, with a total area of approximately 5×10^4 km^2. The TP is also known as the "Water Tower of Asia" [46], which provides water resources for more than a billion people in Asia [47], and more than 50% of China's lakes are located on the TP, which makes the TP an important water resource for China and Asia [10], [48]. The well-known Yangtze River and Yellow River both originate from the TP. The TP is divided into 12 basins by the main rivers, including the Hexi Corridor, Qaidam, Yellow, Yangtze, Mekong, Salween, Inner TP, Tarim, Amu Darya, Indus, Ganges, and Brahmaputra (see Fig. 1).

B. Data

1) GEDI Data: The GEDI is a full waveform lidar altimeter that was launched on 5 December 2018 with an on-orbit checkout in April 2019. The GEDI data were processed and provided by the Land Processes Distributed Active Archive Center (LP DACC), which is attached to the International Space Station (ISS). For the ISS is not maintained in a repeating orbit, GEDI uses an active-track pointing system to help eliminate coverage gaps, which allows more acquisitions and more evenly distribution [33]. The GEDI provides high-quality measurements of the 3-D structure and topography of Earth's forests and terrain between 52°N and 52°S. The GEDI consists of three lasers with a pulse frequency of 242 Hz and one of the lasers' outputs is split into two beams. The two beams with half the power of the full laser and called coverage beams. While the other two lasers remain at full power and are called full-power beams. The coverage lasers fire 5 mJ pulses, while each of the two full power lasers fires 10 mJ pulses [49]. Four beams are dithered across track to produce 8 tracks, which are separated by ∼600 m across the track. The 8 tracks include 4 full power ground tracks (BEAM0101, BEAM0110, BEAM1000,

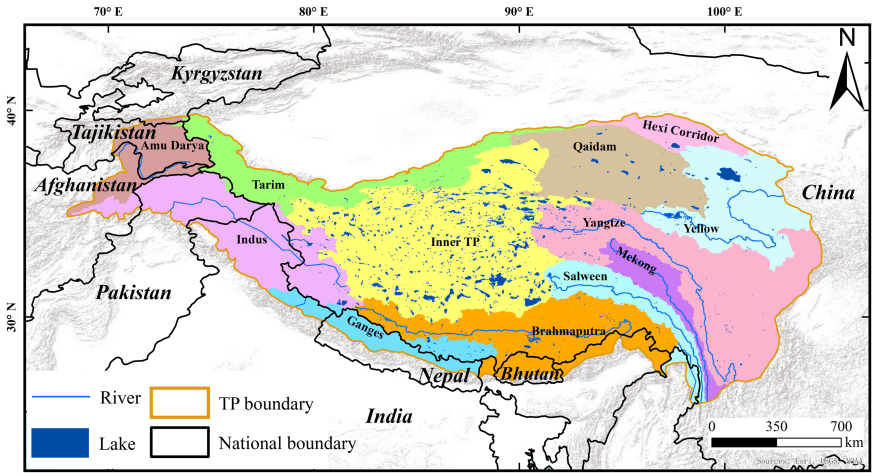

Fig. 1. Geographic map of the lakes on the TP (the 12 basins are shown in different colors).

and BEAM1011) and 4 coverage ground tracks (BEAM0000, BEAM0001, BEAM0010, and BEAM0011). The GEDI has a footprint diameter of ∼25 m and a 60-m distance between footprint centers along the track [34]. The GEDI measures vertical structures using a 1064-nm laser pulse, with a vertical accuracy over relatively flat, nonvegetated surfaces of ∼3 cm [34].

The L1B product provides geolocated, corrected, and smoothed waveforms, geolocation parameters, and geophysical corrections for each laser shot for all eight GEDI beams. The L1B (V002) products from June 2019 to June 2021 were used to extract the instrumental parameters of waveforms (width, amplitude, energy, etc.) for importance analysis. The L2A product provides waveform interpretation and extracted products from each L1B received waveform. The L2A (V002) product from June 2019 to June 2021 was used to calculate the instrumental parameters (signal-to-noise ratio and VAs) for importance analysis. The L2B product mainly extracts biophysical metrics from each GEDI waveform, which provides precise latitude, longitude, elevation, height, and canopy cover data. The L2B (V002) product from June 2019 to June 2021 was used to estimate the lake level on the TP, and the mean time of sampling days tracks for all lake time on the TP in each month from GEDI are shown in Fig. 2. The GEDI products are available from the Earth science data systems of the National Aeronautics and Space Administration (NASA) at https://search.earthdata.nasa.gov/.

2) ICESat-2 Data: The ICESat-2 was launched by NASA on 15 September 2018, with an orbit altitude of 496 km, an orbit inclination of 92°, an orbit repeat period of 91 days [28], and generating 1387 Reference Ground Tracks (RGT) [49], [50]. The laser spot is not perfectly following the RGT for repeated observation, ICESat-2 collects repeat-track observation for the polar region and oceans. The track spacing of the mid-latitudes is larger than the high latitudes, and to measure more forests on the earth, satellites will point slightly off the RGT over land [28], [50]. ICESat-2 carries the enhanced Advanced Topographic Laser Altimeter System (ATLAS), uses photon counting technology, and generates overlapping footprints at a pulse frequency

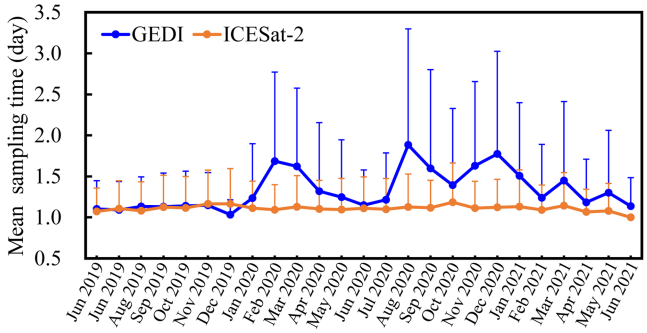

Fig. 2. Mean sampling time of the GEDI and ICESat-2 (denotes the average number of sampling days and standard deviation for lakes on the TP in each month from the GEDI and ICESat-2 from June 2019 to June 2021).

of 10 kHz [50]. The footprint of ICESat-2 is ∼17 m in diameter, samples are obtained at a spacing of approximately 0.7 m along the track, and the accuracy can be up to 0.1 m [51]. ATLAS has six laser tracks, including three strong tracks (GT1R, GT2R, and GT3R) and three weak tracks (GT1L, GT2L, and GT3L) with a wavelength of 532 nm. The transmission energy of the laser pulse of the strong laser tracks is four times that of the weak tracks. The ICESat-2 heights reference the WGS84 ellipsoid and geoid heights reference EGM 2008. ICESat-2 has been widely used to observe the water level of lakes on the TP, and the number of lakes that can be observed by ICESat-2 was also increasing with the increased working time [10], [52], [53]. The Qinghai Lake water level of ICESat-2 compared with the in situ data, the accuracy can reach the centimeter level. [10], [54], [55].

ATL13 was used to estimate the lake level in this study. ATL13 was developed from the ATL03 geolocation photon product, specifically designed for inland water surface height [56]. ATL13 release 003 was used with a minimum segment length of 100 signal photons (over 100 m on average) to obtain lake levels [10]. The ATL13 data on the TP from June 2019 to June 2021 (total 184 RGTs) are available from the National Snow and Ice Data Center at http://nsidc.org/data/icesat/, and

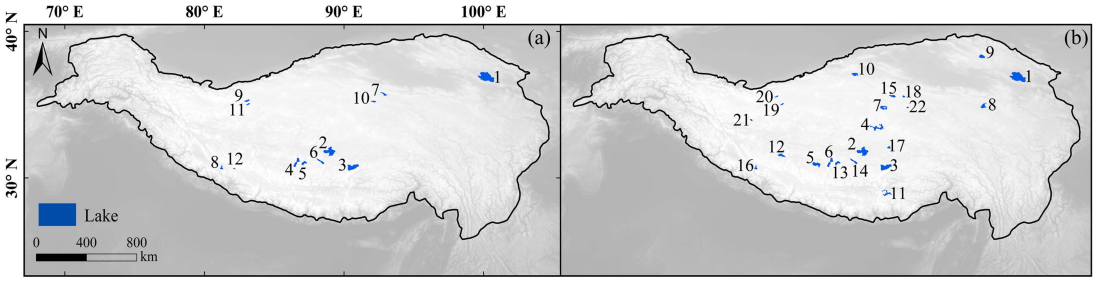

1: Qinghai, 2: Siling-co, 3: Namco, 4: Tangra-yumco, 5: Ngangze 6: Gyaring-co, 7: Kusai, 8: Langa-co, 9: Lashuihe, 10: Courendejia, 11: Bairad, 12: Gongzhu.

1: Qinghai, 2: Siling-co, 3: Namco, 4: Dorsoidong-co, 5: Zhari-namco, 6: Tangra-yumco, 7: Ulan-ul, 8: Ngoring-co, 9: Hala, 10: Aqqikol-hu, 11: Yamzho-yumco 12: Ngangla-ringco, 13: Ngangze, 14: Gyaring-co, 15: Hoh-xil-hu, 16: Langa-co, 17: Zige-tangco, 18: Zonag, 19: Bairad, 20: Heishi-beihu, 20: Gyeze-caka, 21: Telashi.

Fig. 3. Distribution of the DAHITI and Hydroweb datasets (a is the distribution of 12 lakes from the DAHITI dataset, and b is the distribution of 22 lakes from the Hydroweb dataset. The lake names of 12 lakes from DAHITI and 22 lakes from Hydroweb are shown in the figure).

the mean time of sampling days for lakes on the TP in each month from ICESat-2 are shown in Fig. 2.

3) DAHITI and Hydroweb: The Hydrological Time Series of Inland Waters (DAHITI) and Hydroweb datasets were used to compare lake levels with the GEDI and ICESat-2.

DAHITI was developed by the Deutsches Geodätisches Forschungsinstitut der Technischen Universität München (DGFI-TUM) in 2013 to provide a water level time series of inland waters. The lake level of DAHITI is derived from multimission radar altimeters (Sentinel-3A/B and Jason-3 between 2019 and 2021). Twelve lakes on the TP can be found in the DAHITI dataset for comparison (from June 2019 to June 2021), and the spatial distribution is shown in Fig. 3(a). The DAHITI data are available at https://dahiti.dgfi.tum.de/en/.

The Hydroweb dataset was developed by LEGOS/GOHS (Laboratoire d'Etudes en Geophysique et Oceanographie/Equipe Geodesie, Oceanograhie et Hydrologie Spatiale) in France. Hydroweb integrates multimission radar altimeters (Jason-2, Saral/Altika, Sentinel-3, etc.) to provide continuous, long-duration time series of large lake levels with surface areas over 100 km^2 in the world. Twenty-two lakes on the TP can be found in Hydroweb for comparison (from June 2019 to June 2021), and the spatial distribution is shown in Fig. 3(b). The Hydroweb dataset is available at https://hydroweb.theia-land.fr/hydroweb/.

4) Meteorological Factors Derived From ERA5 and MODIS Data: The European Centre for Medium-Range Weather Forecasts provides the fifth generation ECMWF atmospheric reanalysis data (ERA5) from 1979 to present, with a spatial resolution of 0.1° (approximately 10 km). The temperature and wind data for each day on the Google Earth Engine platform (https://code.earthengine.google.com/) from June 2019 to June 2021 were used to analyze the impacts of meteorological factors on lake level differences between GEDI and ICESat-2.

The Moderate Resolution Imaging Spectroradiometer (MODIS) instrument onboard the Earth Observing System Terra and Aqua platforms provided the cloud optical thickness (COT), cloud water content (CWC), and aerosol optical depth (AOD) data and were used to analyze the importance of impact indicators for the differences between the GEDI and ICESat-2. COT is cloud transparency, and it represents how much the cloud prevents light from passing through. CWC is the total amount of liquid or ice water contained in the cloud in a 0.1° $\times$ 0.1° atmospheric column (g/m^2). AOD represents the amount of sunlight that is blocked from reaching the ground due to the presence of aerosol particles, such as dust, haze, or smoke. In this study, MODIS Terra data at an 8-day scale were used, with a spatial resolution of 0.1° (approximately 10 km). The MODIS data are available at https://neo.gsfc.nasa.gov/.

5) Instrument Parameters Derived From the GEDI: Seven instrument parameters were obtained from the GEDI products, including the sensitivity, solar elevation, zcross_amp (represented by Amp), rx_gwidth (represented by width), pulse energy (represented by energy), signal-to-noise ratio (SNR), and viewing angles (VAs), for importance analysis.

Sensitivity is the area of the waveform divided by the area of the total waveform, which can indicate the ground signal detection capability of the waveform. The solar elevation is the elevation of the sun position vector from the laser bounce point position in the local Earth-north up frame [34]. Amp is the amplitude of the lowest mode of the smooth waveform, and width is the received width of the Gaussian fit of the waveform [35]. The received energy with the lowest mode factor was obtained, which can reflect the noise signal of the return waveform [57]. The SNR can express the proportion of the valid signal in the waveform (in dB) [58]. VAs are the angle between the altimeter and footprint point (degree, °), which is mainly determined by the latitude and longitude of the instrument and the footprint [25].

Sensitivity and solar elevation parameters were extracted from the L2B product. Amp and width for each footprint were obtained from the L2A product. The SNR was calculated from the L1B product in (1), and the VAs were calculated from the L2A product in (2)

$$\mathrm{SNR} = 10\log_{10}\left(\frac{A_{\max} - \mu_n}{\sigma_n}\right) \tag{1}$$

where $A_{\max}$ is the maximum amplitude within an acquired waveform (rx_modeamps from L2A); μ_n is the mean background noise (noise_mean from the L1B product); and σ_n is the standard

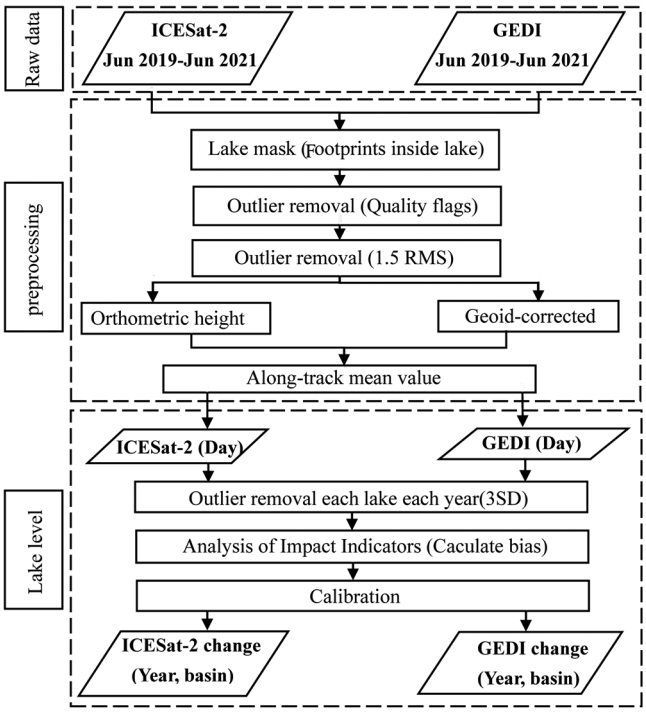

Fig. 4. Flowchart of GEDI and ICESat-2 processing for lake level on the TP.

deviation of the background noise (noise_stddev from the L1B product)

$$\mathrm{VA}_s = \tan^{-1}\frac{d_{si}}{a_i} \tag{2}$$

where d_{si} is the haversine distance between the GEDI shot (s) and the GEDI instrument (i) and a_i is the altitude of the GEDI instrument over the referenced ellipsoid at the shot acquisition time.

C. Lake Level Estimation From the GEDI and ICESat-2

The process of lake level estimation was shown in Fig. 4. First, a lake buffer distance of three times the footprint was set to remove the influence of land disturbance and obtain the altimeter measurements of the GEDI and ICESat-2 inside lakes. The vector file of the TP lake in 2020 used in this article is a dataset of Chinese lakes provided by the National Tibetan Plateau Data Center (https://data.tpdc.ac.cn/), which records the number and area of lakes in China from the 1960s to 2020 [59]. Then, the obvious outliers of altimetry measurements could be removed by the quality flag. For the GEDI and ICESat-2, the quality of the footprint was controlled by filtering the quality flag [56], [57]. GEDI footprints with the "Quality Flag" value equal to 0 were deleted. And GEDI footprints with "algorithmrun_flag" equal to 1, "Stale_retu" equal to 0, and "sensitivity" greater than 0.5 were selected. ICESat-2 footprints with the "qf_bias_fit" value equal to 3/-3 were deleted. And ICESat-2 footprints with "qf_bckgrd" less than 3 and "qf_bias_em" less than 0.05 were selected. Third, the surface elevation of the lake was estimated. Different terrains receive different transmitted energies, and water is usually a lower energy waveform. For the GEDI, the elevation of the lowest mode (ele_lowestmode) was used as the surface lake elevation [36]. The ICESat-2 mainly extracts the orthometric height between the subsatellite point and the altimeter and the significant wave height (SWH). The SWH is defined as the mean value of the three highest waves or four times the standard deviation of surface elevation in each segment in the ATL13 product. The lake surface elevation of each segment was estimated by subtracting the SWH from the orthometric height [10]. Fourth, the outliers of the single-day lake water level were removed. The mode was estimated, which is the elevation bin (step size was 1 m) where most measurements belong to. And the observations outside 1 m of the mode were removed. The root mean square (RMS) and mean lake level of the remaining footprint points were calculated. Footprints were discarded if the absolute value between the observation and the mean lake level were greater than 1.5 RMS. The removal process was continued by repeating the 1.5 RMS step using the mean and RMS of the remaining observations. For the GEDI, the method of 1.5 RMS was stopped when the number of footprints remaining on the track was less than 5. For ICESat-2, the method of 1.5 RMS was stopped when the number of footprints remaining on the track was less than 10 [36], [60], [61]. The mean water level was calculated based on the remaining observations. In addition, the lake levels of both ICESat-2 and GEDI were unified to World Geodetic System 84/Earth Gravity Model 2008 coordinates. Finally, three standard deviations (SD) were used to remove anomalies for each lake and year.

Previous studies using GEDI to retrieve water levels have focused on large lakes and used the three RMS method to remove outliers [36], this study retrieve water levels of all lakes on the TP. Given lakes vary in size on the TP, stricter outlier removal requirements are necessary. The results indicated that the 1.5 RMS method can make the observations of large/small lakes closer to the comparison data. For example, the R^2 between GEDI water level and the DAHITI dataset for Qinghai Lake (approximately 4500 km^2) is 0.90 when using the 1.5 RMS method, compared to 0.88 with the 3 RMS method. Similarly, for Gongzhu Lake (approximately 60 km^2), the R^2 between GEDI water level and the DAHITI dataset is 0.72 with the 1.5 RMS method, compared to 0.71 with the 3 RMS method.

The mean annual water level of each lake was calculated separately for GEDI and ICESat-2, which is equal to the average daily water level for the year (3). The mean annual water level change is equal to the average water level of the subsequent year minus the average water level of the previous year

$$L_{year(j)} = \frac{\sum_i^t L_{day(i)}}{t} \tag{3}$$

$$\Delta L_{year} = L_{year(j)} - L_{year(j-1)} \tag{4}$$

where $L_{year(j)}$ is the mean annual water level of one lake in j year, $L_{day(i)}$ is the lake level at i day. t is the number of days of the lake in j year. ΔL_{year} is the mean annual water level change of one lake from j year to $j-1$ year, $L_{year(j-1)}$ is the mean water of the lake in $j-1$ year.

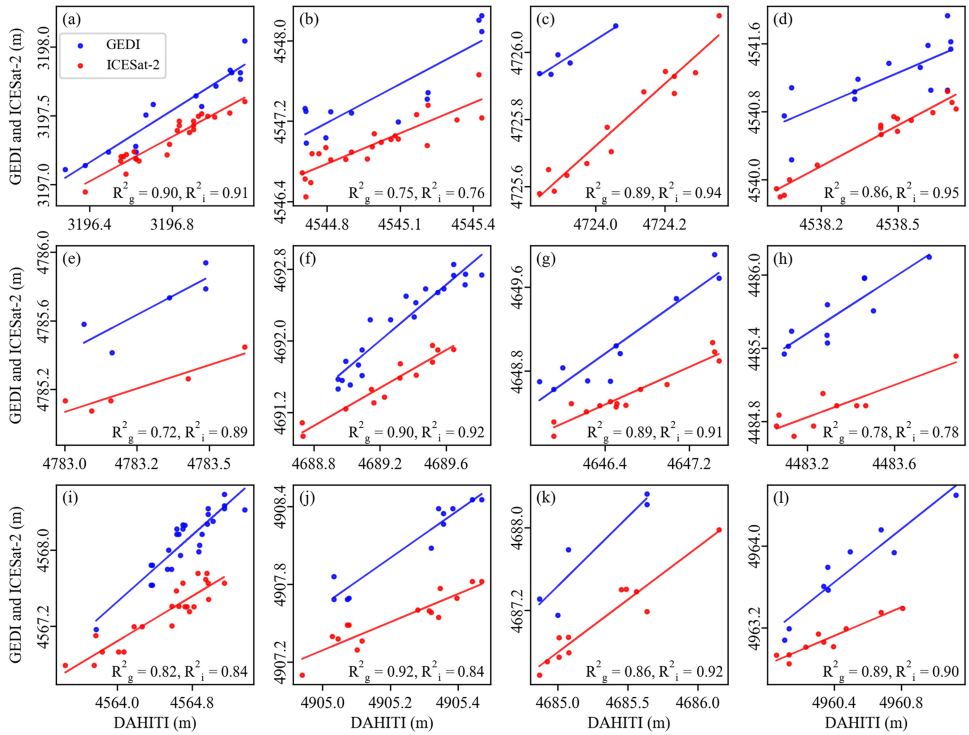

Fig. 5. Linear fitting results of the GEDI and ICESat-2 water levels with the water level of 12 lakes from the DAHITI dataset (figures a to l are the linear results between 12 lakes and DAHITI, and the lake location can be found in Fig. 3(a). R^2_g is the coefficient of determination between the GEDI and DAHITI, and R^2_i is the coefficient of determination between the ICESat-2 and DAHITI).

D. Comparison of Lake Levels

The lake level between GEDI and ICESat-2 of 18 sample lakes for the most recent day within ten days were selected for comparison. The lake level between comparison datasets (DAHITI and Hydroweb) and lake level of estimation (GEDI and ICESat-2) for the most recent day within ten days were selected. Each lake should have at least four water levels of comparison data. Four statistical metrics were used to evaluate the performance of altimeter measurements, including the coefficient of determination (R^2), root mean square error (RMSE), and standard deviation (SD). These metrics were used in similar studies [6], [10], [36].

E. Analysis Method of Impact Indicators

Seven instrument parameters and five meteorological factors affecting the GEDI water level inversion error were selected and calculated, including sensitivity, solar altitude, Amp, width, pulse energy, SNR, VAs, air temperature, wind, COT, CWC, and AOD. In the relative importance analysis, the water level of ICESat-2 was considered to be the ground truth value. The relative importance of the indicators affecting the difference between the GEDI and ICESat-2 can be obtained by using random forest regression model analysis. The random forest model can calculate a parameter called the percent increase in mean squared error (%IncMSE) to determine the relative importance of each input variable; the higher the %IncMSE value is, the more important the input factor is [62], [63].

F. Calibration Between the GEDI and ICESat-2

To calibrate the bias between the GEDI and ICESat-2, lake levels from the GEDI and ICESat-2 within 10 days for all lakes on the TP were selected. The mean bias was calculated mainly from the instrument. The importance values obtained from the random forest regression model analysis were normalized. The important value of instrument parameters accounted for more than 50% of the lake's total importance values, the mean bias of this part was calculated. After calibrating the bias between the GEDI and ICESat-2, the water levels were combined. Finally, the lake level was a sequence of two altimeters. In addition, when the GEDI and ICESat-2 had water levels on the same day, the lake level of ICESat-2 was reserved.

III. Results

A. Comparisons of Lake Levels Derived From the GEDI and ICESat-2 With DAHITI and Hydroweb Datasets

Both the GEDI and ICESat-2 agreed with the DAHITI and Hydroweb datasets, while the ICESat-2 had an overall higher accuracy than the GEDI. In the 12 lakes provided by DAHITI, the GEDI had an average R^2 of 0.85 (ranging from 0.72 to 0.92) and 0.88 (ranging from 0.76 to 0.95) for the ICESat-2 (see Fig. 5). The 22 lakes provided by Hydroweb showed that the GEDI had an average R^2 of 0.81 (ranging from 0.70 to 0.97) and 0.86 (ranging from 0.72 to 0.95) for the ICESat-2 (see Fig. 6). Comparison of GEDI with ICESat-2 for 18 lakes showed that the GEDI had an average R^2 of 0.87, and ranging from 0.80

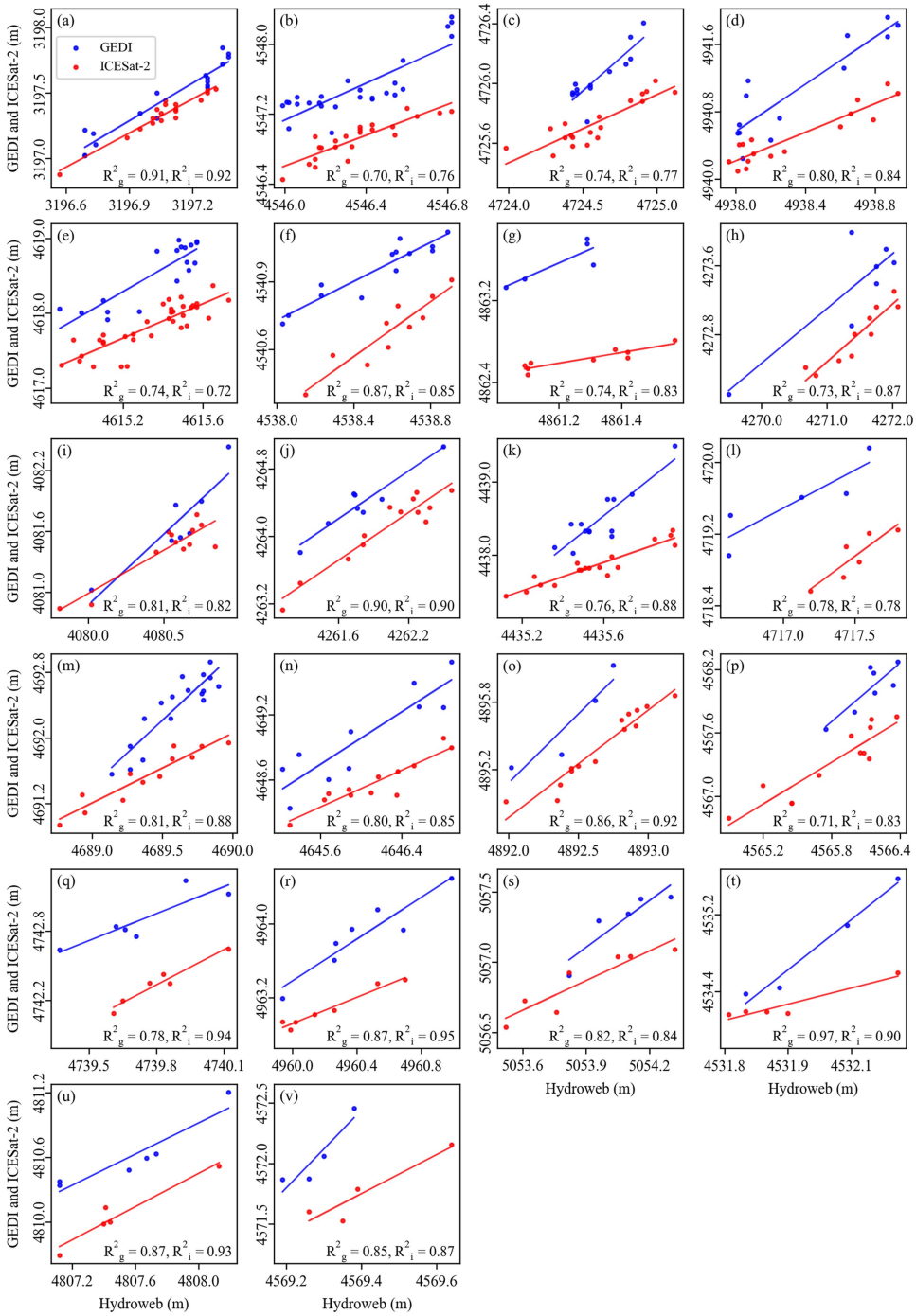

Fig. 6. Linear fitting results of the GEDI and ICESat-2 water levels with water levels for 22 lakes from the Hydroweb dataset (figures a to v are the linear results between 22 lakes and Hydroweb; the lake locations can be found in Fig. 3(b). R^2_g is the coefficient of determination between the GEDI and Hydroweb, and R^2_i is the coefficient of determination between the ICESat-2 and Hydroweb).

to 0.98 (see Fig. 7). Qinghai Lake is the largest lake on the TP, and it showed good fitting results with both the DAHITI and Hydroweb datasets. The fitting results of the GEDI and ICESat-2 with DAHITI in Qinghai Lake showed that the R^2 values were 0.90 ($P < 0.01$) and 0.91 ($P < 0.01$), RMSEs were 0.54 and 0.50 m, and SDs were 0.28 and 0.16 m, respectively. The fitting results of the GEDI and ICESat-2 with Hydroweb in Qinghai Lake showed that the R^2 values were 0.91 ($P < 0.01$) and 0.92 ($P < 0.01$), RMSEs were 0.38 and 0.28 m, and SDs were 0.26 and 0.15 m, respectively. The fitting results of the GEDI and ICESat-2 in Qinghai Lake showed that the R^2 values were 0.91 ($P < 0.01$), RMSE were 0.36 m and SDs were 0.23 m. The GEDI performs well for the water level on the TP, and the RMSE was only 0.23 m of the GEDI water level in Qinghai Lake compared with the ICESat-2 result by Zhang et al. [10], in which the RMSE was 0.1 m compared with in situ measurements in Qinghai Lake.

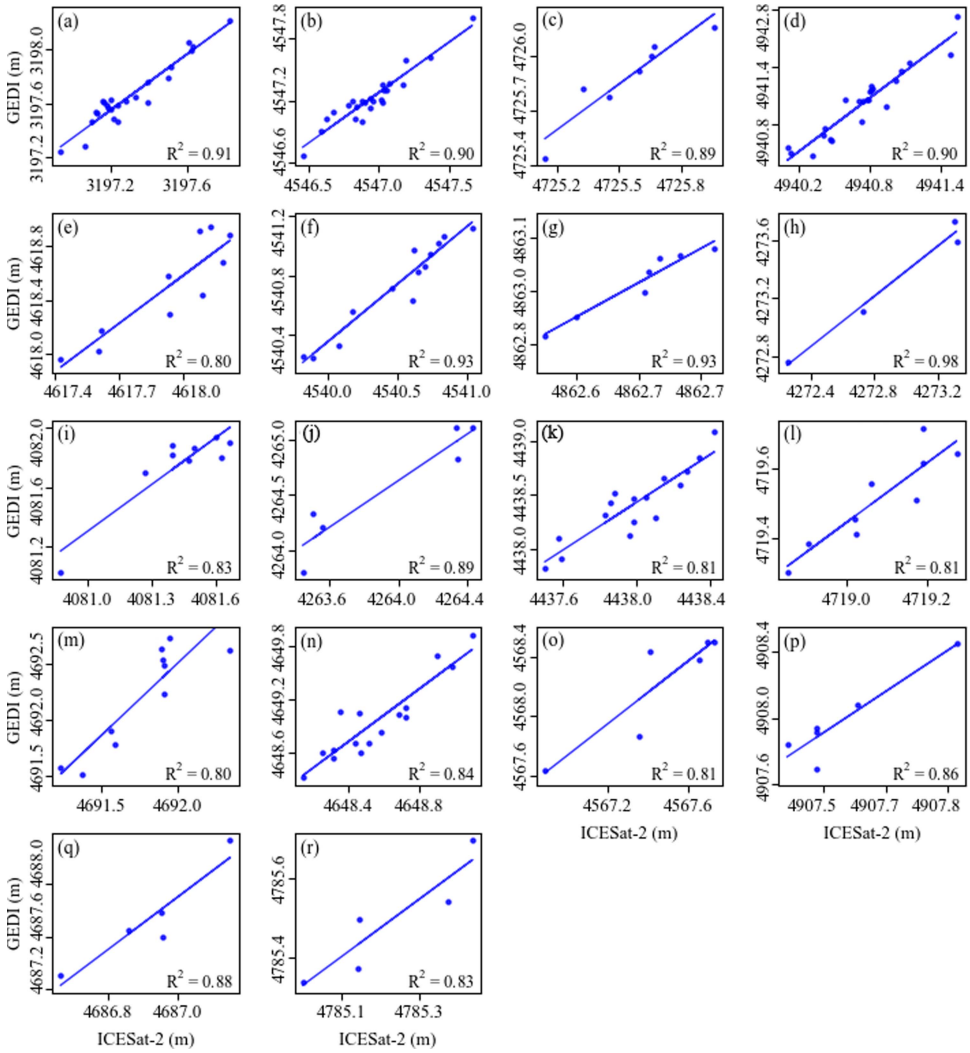

Fig. 7. Linear fitting results of the GEDI and ICESat-2 water levels for 18 lakes (figures a to r are the linear results between GEDI and ICESat-2; the lake locations can be found in Fig. 3. R^2 is the coefficient of determination between the GEDI and ICESat-2).

B. Spatial Distribution of Lakes Observed By the GEDI and ICESat-2

From June 2019 to June 2021, the GEDI and ICESat-2 can cover more than half of the lakes on the TP, respectively. While the lake coverage of the GEDI was much greater than that of the ICESat-2. When the number of days of the lake water level was greater than or equal to 1, the GEDI obtained the water level of 1882 lakes (97.61% on the TP), and ICESat-2 obtained the water level of 1112 lakes (57.68%). The number of lakes estimated by the GEDI was much greater than that previously estimated by the Cryosat-2 or ICESat-2 [10], [64]. The GEDI obtained 39.93% (770) more lakes than the ICESat-2, and 1092 (56.64%) lakes were obtained by both the GEDI and ICESat-2. When the water level was available for at least one day in each of the three years (in 2019, 2020, and 2021). The GEDI obtained water levels for 755 lakes (39.16%) [see Fig. 8(c)], and 544 lakes were in the Inner Plateau basin [see Fig. 8(b)]. The GEDI obtained 330 more lakes than the ICESat-2, and 300 lakes were obtained by both the GEDI and ICESat-2 [see Fig. 8(c)]. The GEDI and ICESat-2 were similarly distributed on the TP, and the spatial coverage of the GEDI was more extensive, especially in the northwestern part of the Inner Plateau and the northwestern part of the Yangtze basin [see Fig. 8(a)]. The 300 lakes obtained by both the GEDI and ICESat-2 were mainly concentrated in the Inner Plateau basin and the Yangtze and Brahmaputra basins [see Fig. 8(a)].

C. Analysis of the Difference in Lake Levels Between the GEDI and ICESat-2

A total of 245 lakes were selected for analysis based on lake level results from the GEDI and ICESat-2, and the 245 lakes were obtained by both the GEDI and ICESat-2 (total 300 lakes) after removing the missing indicators. The difference in lake levels came from a variety of indicators, and 12 indicators were collected to analyze the lake level difference between the GEDI and ICESat-2, including seven instrument parameters (sensitivity, width, Amp, SNR, VAs, energy, and solar elevation) and five meteorological factors (air temperature, wind, COT,

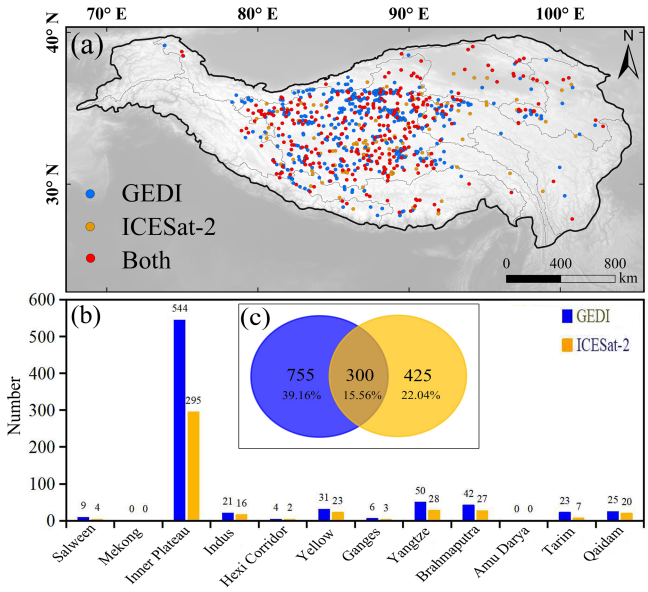

Fig. 8. Spatial distribution and statistics of the lakes [(a) is the distribution of lakes with three years of water levels (2019, 2020, and 2021) obtained by the GEDI, ICESat-2, and both altimeters, respectively; (b) is the number of lakes in different basins; (c) is the number of lakes covered by the GEDI and ICESat-2, respectively.].

CWC, and AOD.). In addition, different properties were used to analyze the differences between the GEDI and ICESat-2, such as different lake areas, basins, and beams.

The random forest importance analysis was carried out on the 245 lakes after removing the missing indicator, and 12 impact indicators were ranked. The results showed that two instrument parameters (VAs and solar elevation) and one meteorological factor (air temperature and wind) were the four important indicators of single lake water level differences between the GEDI and ICESat-2. VA was the most important indicator for 22.86% of the lakes, followed by air temperature solar elevation and wind, which were the most important indicators for 15.51%, 14.69%, and 13.88% of the lakes, respectively. Most of the indicators accounted for less than 30% of the importance ranking, and only three meteorological factors accounted for more than 30% of the importance ranking, namely, COT (37.96% in the eleventh rank), CWC (38.37% in the tenth rank), and AOD. AOD had the least effect on the difference between the GEDI and ICESat-2, with AOD being the least important indicator in the ranking in 87.35% of the lakes.

The relative importance of each impact indicator has different effects on lake level differences under different lake areas, basins, and beams. The results showed that, except for VAs and solar elevation, meteorological factors (air temperature, CWC, COT, and AOD) had a greater effect on the difference than instrument parameters (sensitivity, width, Amp, SNR, and energy) (Figs. 9–11). Four indicators (VAs, solar elevation, air temperature, and wind) showed high importance in different lake areas, basins, and beams (Figs. 9–11). The importance of impact indicators was relatively balanced in the lake from 1 to 10 km^2 [see Fig. 9(a)]. The impact of the indicators was more obvious in the lakes with an area larger than 100 km^2 [see Fig. 9(c)–(e), and Fig. 7(f)] and the importance of wind was more obvious when the lake area was larger than 50 km^2 [see Fig. 9(b)–(f)]. VAs was an important indicator for the lake level difference for different area ranges, with the importance reaching a maximum for areas larger than 1000 km^2 [see Fig. 9(f)].

The importance of indicators showed different characteristics in different basins. VAs, solar elevation, air temperature, and wind were the most important in the Inner Plateau basin [see Fig. 10(b)]. VAs were the most important indicator in the Salween, Inner Plateau, Yellow, and Tarim basins [see Fig. 10(a), (b), (e), and (i)]. In the Indus, Hexi Corridor, Ganges, Yangtze, Brahmaputra, and Qaidam basins, solar elevation was more important than VAs [see Fig. 10(c), (d), (f), (g), and (h)], and (j)]. The important value of wind ranked among the top four in each basin, but was lower in Ganges than other basins [see Fig. 10(f)]. The importance of each indicator for the eight GEDI beams was similar, with the full power beams having slightly higher importance values than the coverage beams [see Fig. 11(e)–(h)].

D. Lake Levels Obtained By Combining the GEDI and ICESat-2

After calibrating the instrument bias (0.33 m) between the GEDI and ICESat-2, the lake levels of these two altimeters were combined. Water levels of 921 lakes (789 lakes of the 921 lakes >1 km^2) were obtained, with all lake levels from 2019, 2020, and 2021. The lakes were distributed in 11 basins; the Inner Plateau basin had the most lakes at 639, and the Mekong had only 3 lakes. The water level change of 789 lakes on the Tibetan Plateau ranged from -0.98 to 0.97 m from 2019 to 2020 (see Table I). The lakes in the Inner Plateau showed complex changes, with the largest change ranging from -0.98 to 0.94 m from 2019 to 2020 (see Table I). From 2020 to 2021, the water level on the TP varied between -0.98 and 0.93 m, with the greatest fluctuation occurred in the Yangtze basin. Spatially, the regions with increased lake levels were mainly concentrated in the Inner Plateau and the northern TP (Qaidam, Hexi Corridor, and north of the Yangtze basin) from 2019 to 2020 [see Fig. 12(a)]. Lake level drops were sporadic occurrences on the Inner Plateau [see Fig. 12(a)]. The regions where the lake level has dropped were mainly concentrated in the Indus, Ganges, and Brahmaputra basins (see Fig. 12), which was consistent with the 32° N dividing line [65].

IV. Discussion

The DAHITI and Hydroweb datasets have been widely used in hydrological studies. The water level provided by DAHITI and Hydroweb was not only for long-term water level studies [66], [67], but also for the study of water level comparative [10], [68], [69]. Especially for long-term water level studies, DAHITI and Hydroweb datasets were more reliable [66]. The accuracy of DAHITI in large lakes was better than in small lakes, with an RMSE of 4–5 cm [70]. Compared with the in situ data, the accuracy of Hydroweb lakes/reservoirs was 5–24 cm [69]. The DAHITI and Hydroweb are ideal basic datasets for the TP, which lacks in-situ measurements. The R^2 value between the in-situ of Qinghai Lake and the water level composed of DAHITI and

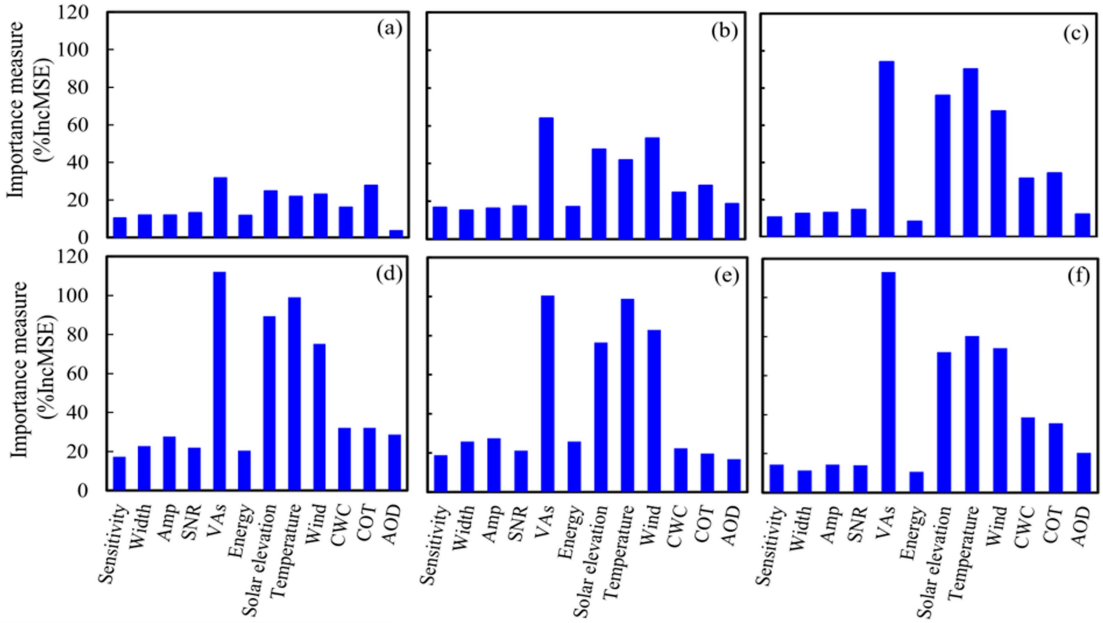

Fig. 9. Relative importance (measured as %IncMSE) of impact indicators for lake level differences between the GEDI and ICESat-2 in different lake areas. [(a) is 1–10 km^2, (b) is 10–50 km^2, (c) is 50–100 km^2, (d) is 100–500 km^2, (e) is 500–1000 km^2, and (f) is greater than 1000 km^2].

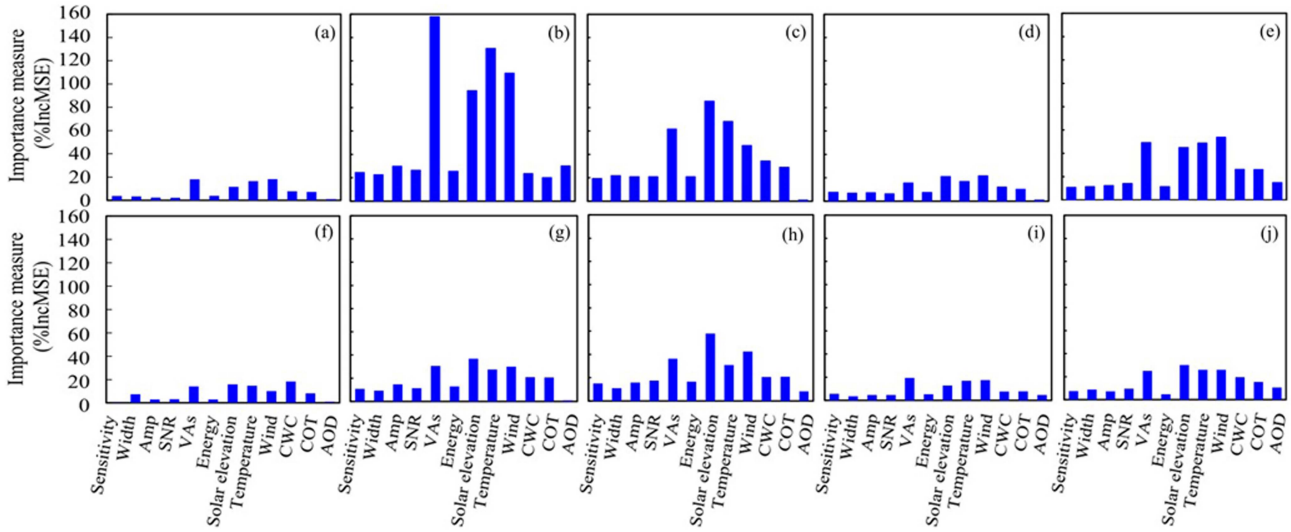

Fig. 10. Relative importance (measured as %IncMSE) of impact indicators for lake level differences between the GEDI and ICESat-2 in different basins [(a) is the Salween, (b) is the Inner Plateau, (c) is the Indus, (d) is the Hexi Corridor, (e) is the Yellow, (f) is the Ganges, (g) is the Yangtze, (h) is the Brahmaputra, (i) is the Tarim, and (j) is the Qaidam].

Hydroweb was 0.90 [66]. The R^2 between the Hydroweb and lakes (Selin Co, Nam Co, and Tang-ro Yum Co) on the TP were all great than 0.8 [69], which was similar to the results in this study.

The lake level monitoring of the ICESat-2 on the TP has been demonstrated to be accurate, reaching the centimeter level [10], [52]. Many studies have shown that the accuracy of the ICESat-2 was slightly higher than that of the GEDI [17], [36], which was also confirmed in this study. Comparing the GEDI with in situ data, the average RMSE was 0.21 m for eight lakes in Switzerland [35], 0.28 m for the Great Lakes, and 0.40 m for the lower Mississippi River [36]. Due to the instrument altimeter bias and geoid variations in the comparison dataset [3], [32], the DAHITI and Hydroweb average RMSE of the GEDI was 0.46 m on the TP, and the accuracy of the GEDI was acceptable. Naturally, GEDI data can be more accurate in estimating lake levels when using machine learning models [37]. The common methods used in the calibration process of multisource satellites are mean bias calibration (constant calibration) and linear calibration. The constant calibration was more commonly used in water level combinations with multisource satellites, while linear calibration was used for water level of long time series [13], [71]. The calibration method used in this study is a similar mean bias calibration mainly from the

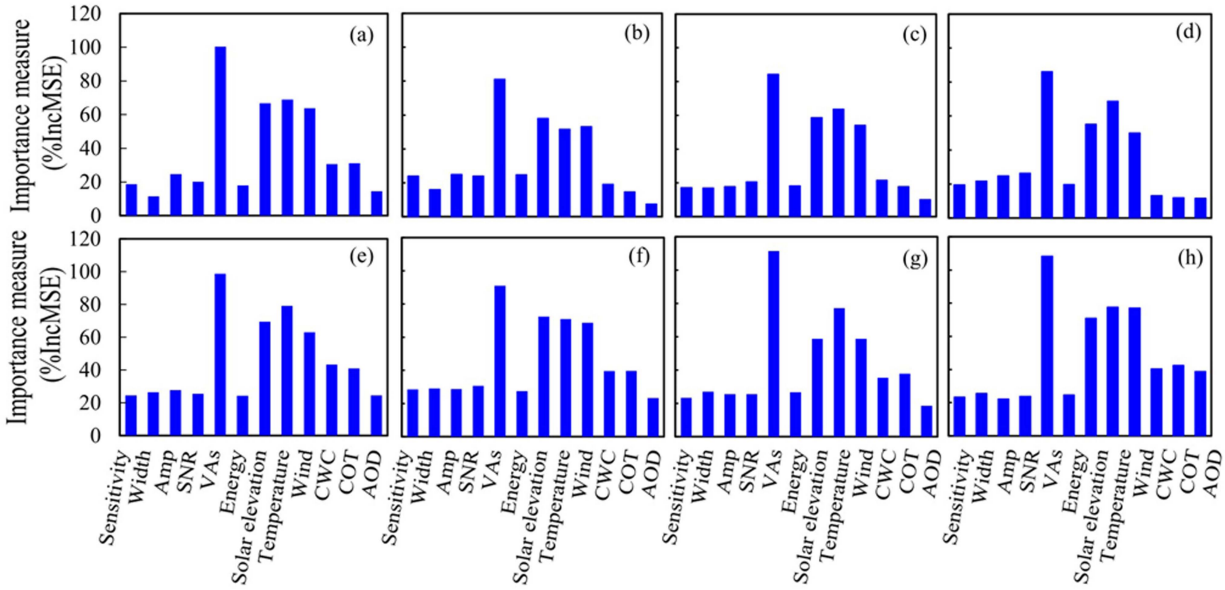

Fig. 11. Relative importance (measured as %IncMSE) of impact indicators for lake level differences between the GEDI and ICESat-2 of different beams. [(a)–(c), and (d) are coverage beams, and (e)–(h) are power beams].

TABLE I
LAKE LEVEL CHANGES IN DIFFERENT BASINS

		2019-2020			2020-2021		
Basin	Number	Max	Min	Range	Max	Min	Range
Inner Plateau	552	0.94	−0.98	1.92	0.78	−0.92	1.70
Yangtze	53	0.97	−0.79	1.76	0.93	−0.84	1.77
Brahmaputra	49	0.67	−0.83	1.50	0.87	−0.61	1.48
Yellow	41	0.84	−0.98	1.82	0.92	−0.75	1.67
Qaidam	26	0.92	−0.68	1.60	0.9	−0.54	1.44
Indus	25	0.38	−0.97	1.35	0.66	−0.42	1.08
Tarim	17	0.62	−0.90	1.52	0.56	−0.98	1.54
Salween	11	0.56	−0.90	1.46	0.53	−0.46	0.99
Ganges	9	0.53	−0.49	1.02	0.22	−0.81	1.03
Hexi Corridor	3	0.11	−0.29	0.40	0.16	−0.57	0.73
Mekong	2	0.30	−0.32	0.62	0.37	−0.6	0.97
Total	789	0.97	−0.98	1.95	0.93	−0.98	1.91

instrument. There was an almost parallel relationship between the water levels of GEDI and ICESat-2 (see Fig. S1), as well as a good linear relationship between GEDI and ICESat-2 (see Fig. 6). The constant calibrated and linear calibrated water levels were similar, with 18 examples showing R^2 greater than 0.8 for constant calibrated and linear calibrated water levels, and an average RMSE of 0.13 m (see Fig. S2). Finally, water level of 921 lakes were obtain by combined the GEDI and ICESat-2. The combined water level result of 18 lakes were showed in Figure S3. The lake level change was similar to previous study on the TP [16], [65]. Changes in lake level were affected by high spatial heterogeneity; precipitation was the main reason for the increase in lake level, and glacial meltwater in the Inner Plateau provided an additional water supply [8], [65], which led to the rise in lake water level.

The VAs, solar elevation, air temperature, and wind are the main impact indicators of the difference between the GEDI and ICESat-2. The VA values can directly reflect the angular relationship between the footprint point and the altimeter, which is the most important indicator in importance ranking. Fayad [25] also showed that the VAs were the most important indicator for lake level accuracy over the five North American Great Lakes. Laser altimeters are sensitive to photon signals, especially during the day or night [35], and different solar elevations represent different times, different solar backgrounds, and atmospheric scattering, directly affecting water level inversion. At higher

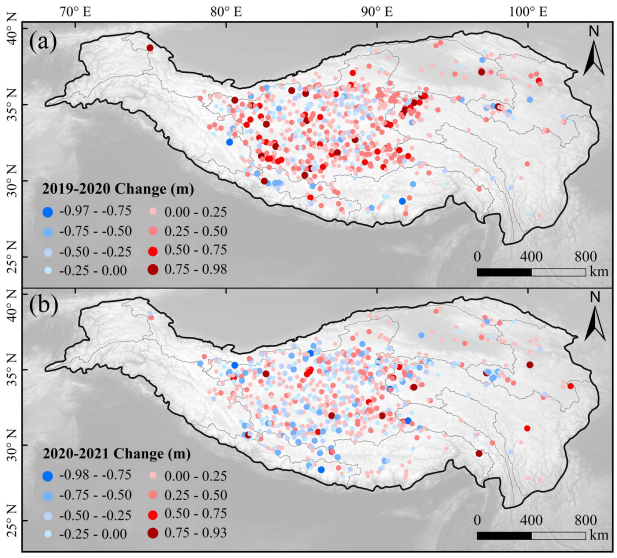

Fig. 12. Lake level changes on the TP from 2019 to 2021 [(a) is lake level change in lake areas greater than 1 km^2 from 2019 to 2020, (b) is lake level change in lake areas greater than 1 km^2 from 2020 to 2021].

temperatures, small currents generated by thermal effects can also affect the waveform, resulting in reduced accuracy and increased bias [72]. The accuracy of the water level was affected by the wind-generated waves and seiches [35]. AOD being the least important indicator perhaps because the TP is located far from human activity [4]. The full power beams have stronger energy and density than the coverage beams. Under the interaction of the two beams, the coverage beam was more susceptible to being affected [36], so the full power beam was more stable than the coverage laser beam. There were some unavoidable uncertainties in the analysis of the differences between the GEDI and ICESat-2, such as the uncertainty of time and the influence factor, because the difference between the two data was due to the deviation of the lake level within ten days. In addition, most of the impact indicators came from the results of the model estimates, and there were deviations from the actual measurements.

From June 2019 to June 2021, our results showed that GEDI covered more lakes than ICESat-2 on the TP. However, the fact that there are some design differences between the two altimeters cannot be avoided. The observation orbits between the GEDI and ICESat-2 are different. ICESat-2 follows the RGT for repeated observation, but it does not collect repeat-track in all regions of the earth. To measure more forests on the earth, ICESat-2 will point slightly off the RGT over land at mid and low latitudes [49], [50]. The latitude where the TP is located performs an off-pointing observation strategy, and the lake location and size determine the frequency of ICESat-2 observation [53]. GEDI is attached to the ISS track, which is not a repeating track. To make more measurements on the earth, GEDI uses an active-track pointing system [33], which also allows more lakes to be observed. In addition, GEDI and ICESat-2 have different numbers of lasers and ground tracks. The ICESat-2 has one laser and six tracks, while the GEDI has three lasers and eight tracks, which is currently the largest number of lasers and observation tracks for the altimeter. More tracks can observe more lakes. With increased working times of altimeters and the combination of multiple altimeters that allow for improved spatial and temporal resolutions, altimeters have great potential for monitoring more lakes on the TP.

V. Conclusion

In this study, the GEDI and ICESat-2 were used to estimate lake levels on the TP from June 2019 to June 2021. The accuracy of the GEDI and ICESat-2 was compared, and the impact indicators of the differences between the GEDI and ICESat-2 were discussed. A lake level dataset was obtained by combining the GEDI and ICESat-2.

The GEDI performed well in estimating lake levels on the TP. The 12 lakes provided by DAHITI and the 22 lakes provided by Hydroweb showed that the GEDI and ICESat-2 had an average R^2 greater than 0.8. The RMSE values of the Qinghai Lake GEDI between DAHITI and Hydroweb were 0.54 and 0.38, respectively. In addition, the RMSE values of the Qinghai Lake ICESat-2 between DAHITI and Hydroweb were 0.50 and 0.28, respectively. As the latest lidar altimeter, the GEDI was suitable for lake level inversion, but the accuracy of the ICESat-2 was slightly higher than that of the GEDI.

The GEDI can obtain the water levels of more lakes than the ICESat-2. The number of lakes obtained by the GEDI was 39.93% (770) greater than that of the ICESat-2, and they were mainly concentrated in the Inner Plateau basin. Three hundred lakes were obtained by both the GEDI and ICESat-2. The differences in lake level inversions between the GEDI and ICESat-2 were mainly caused by VAs, solar elevation, air temperature, and wind. Overall, meteorological factors (air temperature, wind, COT, CWC, and AOD) were more important than instrument parameters (sensitivity, width, Amp, SNR, VAs, energy, and solar elevation) in different lake areas, basins or beams. From June 2019 to June 2021, the combination of the GEDI and ICESat-2 provided the water level monitoring results of 921 lakes on the TP. In 2019–2020 and 2020–2021, the largest water level change range of 789 lakes (>1 km^2, in the part of 921 lakes) was mainly in the Inner Plateau and the Yangtze basin. Increases occurred mainly in the Hexi Corridor, Qaidam, Yangtze, and Inner Plateau basins, and decreases occurred in the Ganges and Brahmaputra basins.

Although the data released by the GEDI at this stage are still very limited and some impact indicators cannot be accurately provided, with the comprehensive utilization of multisource altimetry data, an increasing number of lakes could be observed, and the mechanism of lake changes on the TP is expected to be further understood. In addition, with data improvement, the comprehensive indicators and improvement in lake surface water accuracy are expected to be comprehensively studied.

Acknowledgment

The authors would like to thank the LP DACC and NASA for GEDI, ICESat-2, and MODIS data, the DGFI-TUM for DAHITI dataset, the LEGOS/GOHS for Hydroweb dataset, and the ECMWF for ERA5 datasets.

REFERENCES

[1] W. S. Robert, K. Bonnie, P. Stephen, P. Rajendra, R. Kirsten, and R. Maggie, "Ecosystem services of Earth's largest freshwater lakes," *Ecosyst. Serv.*, vol. 41, 2020, Art. no. 101046, doi: 10.1016/j.ecoser.2019.101046.

[2] R. I. Woolway and C. J. Merchant, "Worldwide alteration of lake mixing regimes in response to climate change," *Nature Geosci.*, vol. 12, no. 4, pp. 271–276, 2019, doi: 10.1038/s41561-019-0322-x.

[3] J. F. Crétaux et al., "Lake volume monitoring from space," *Surv. Geophys.*, vol. 37, no. 2, pp. 269–305, 2016, doi: 10.1007/s10712-016-9362-6.

[4] J. F. Pekel, A. Cottam, N. Gorelick, and A. S. Belward, "High-resolution mapping of global surface water and its long-term changes," *Nature*, vol. 540, no. 7633, pp. 418–422, 2016, doi: 10.1038/nature20584.

[5] R. Adrian et al., "Lakes as sentinels of climate change," *Limnol. Oceanogr.*, vol. 54, no. 2/6, pp. 2283–2297, 2009, doi: 10.4319/lo.2009.54.6_part_2.2283.

[6] Y. Cai, C. Q. Ke, and X. Shen, "Variations in water level, area and volume of Hongze Lake, China from 2003 to 2018," *J. Great Lakes Res.*, vol. 46, no. 6, pp. 1511–1520, 2020, doi: 10.1016/j.jglr.2020.08.024.

[7] Y. Yin, Y. Chen, S. Yu, W. Xu, W. Wang, and Y. Xu, "Maximum water level of Hongze Lake and its relationship with natural changes and human activities from 1736 to 2005," *Quaternary Int.*, vol. 304, pp. 85–94, 2013, doi: 10.1016/j.quaint.2012.12.042.

[8] L. Jiang, K. Nielsen, O. B. Andersen, and P. Bauer-Gottwein, "CryoSat-2 radar altimetry for monitoring freshwater resources of China," *Remote Sens. Environ.*, vol. 200, pp. 125–139, 2017, doi: 10.1016/j.rse.2017.08.015.

[9] D. M. Hannah et al., "Large-scale river flow archives: Importance, current status and future needs," *Hydrological Processes*, vol. 25, no. 7, pp. 1191–1200, 2011, doi: 10.1002/hyp.7794.

[10] G. Zhang, W. Chen, and H. Xie, "Tibetan Plateau's lake level and volume changes from NASA's ICESat/ICESat-2 and landsat missions," *Geophysical Res. Lett.*, vol. 46, no. 22, pp. 13107–13118, 2019, doi: 10.1029/2019GL085032.

[11] C. M. Birkett, "The contribution of TOPEX/POSEIDON to the global monitoring of climatically sensitive lakes," *J. Geophysical Res., Oceans*, vol. 100, no. C12, pp. 25179–25204, 1995, doi: 10.1029/95JC02125.

[12] J. F. Crétaux et al., "SOLS: A lake database to monitor in the near real time water level and storage variations from remote sensing data," *Adv. Space Res.*, vol. 47, no. 9, pp. 1497–1507, 2011, doi: 10.1016/j.asr.2011.01.004.

[13] X. D. Li, D. Long, Q. Huang, P. F. Han, F. Y. Zhao, and Y. Wada, "High-temporal-resolution water level and storage change data sets for lakes on the Tibetan Plateau during 2000-2017 using multiple altimetric missions and Landsat-derived Lake shoreline positions," *Earth System Sci. Data*, vol. 11, no. 4, pp. 1603–1627, 2019, doi: 10.5194/essd-11-1603-2019.

[14] J. J. Liao, H. Xue, and J. M.Chen, "Monitoring lake level changes on the Tibetan Plateau from 2000 to 2018 using satellite altimetry data," *J Remote Sens. (Chinese)*, vol. 24, no. 12, pp. 1534–1547, 2020, doi: 10.11834/jrs.20209281.

[15] M. R. Suryawanshi, S. Chander, S. R. Oza, and I. M. Bahuguna, "Variability in the ice sheet elevations over Antarctica derived from repetitive SARAL/AltiKa radar altimeter data (2013–2016)," *J. Earth Syst. Sci.*, vol. 128, 2019, Art. no. 64, doi: 10.1007/s12040-019-1093-x.

[16] G. Q. Zhang et al., "Response of Tibetan Plateau lakes to climate change: Trends, patterns, and mechanisms," *Earth-Sci. Rev.*, vol. 208, 2020, Art. no. 103269, doi: 10.1016/j.earscirev.2020.103269.

[17] F. Frappart, F. Blarel, I. Fayad, M. Bergé-Nguyen, and N. Baghdadi, "Evaluation of the performances of radar and lidar altimetry missions for water level retrievals in mountainous environment: The case of the swiss lakes," *Remote Sens.*, vol. 13, no. 11, 2021, Art. no. 2196, doi: 10.3390/rs13112196.

[18] B. E. Schutz, H. J. Zwally, C. A. Shuman, D. Hancock, and J. P. DiMarzio, "Overview of the ICESat mission," *Geophysical Res. Lett.*, vol. 32, 2005, Art. no. L21S01, doi: 10.1029/2005GL024009.

[19] C. Song, Q. Ye, and X. Cheng, "Shifts in water-level variation of namco in the central Tibetan Plateau from ICESat and Cryosat-2 altimetry and station observations," *Sci. Bull.*, vol. 60, no. 14, pp. 1287–1297, 2015, doi: 10.1007/s11434-015-0826-8.

[20] X. Shen, C. Q. Ke, Q. Wang, J. Zhang, L. Shi, and X. Zhang, "Assessment of Arctic Sea ice thickness estimates from ICESat-2 using Icebird airborne measurements," *IEEE Trans Geosci. Remote Sens* ., vol. 59, no. 5, pp. 3764–3775, May 2021, doi: 10.1109/TGRS.2020.3022945.

[21] R. Kwok et al., "Surface height and sea ice freeboard of the Arctic Ocean-from ICESat-2: Characteristics andearly results," *J. Geophysical Res., Oceans*, vol. 124, pp. 6942–6959, 2019, doi: 10.1029/2019JC015486.

[22] S. Nandy, R. Srinet, and H. Padalia, "Mapping forest height and above-ground biomass by integrating ICESat-2, Sentinel-1 and Sentinel-2 data using random forest algorithm in Northwest Himalayan foothills of India," *Geophysical Res. Lett.*, vol. 48, no. 14, 2021, Art. no. e2021GL093799, doi: 10.1029/2021GL093799.

[23] C. Hilbert and C. Schmullius, "Influence of surface topography on ICESat/GLAS forest height estimation and waveform shape," *Remote Sens.*, vol. 4, no. 8, pp. 2210–2235, 2012, doi: 10.3390/rs4082210.

[24] Y. Fan, C. Q. Ke, X. Zhou, X. Shen, X. Yu, and D. Lhakpa, "Glacier mass-balance estimates over high Mountain Asia from 2000 to 2021 based on ICESat-2 and NASADEM," *J. Glaciol.*, pp. 1–13, 2022, doi: 10.1017/jog.2022.78.

[25] I. Fayad, N. Baghdadi, and F. Frappart, "Comparative analysis of GEDI's elevation accuracy from the first and second data product releases over inland waterbodies," *Remote Sens.*, vol. 14, no. 2, 2022, Art. no. 340, doi: 10.3390/rs14020340.

[26] N. N. Baghdadi, M. El Hajj, J. S. Bailly, and F. Fabre, "Viability statistics of GLAS/ICESat data acquired over tropical forests," *IEEE J. Sel. Topics Appl. Earth Observ. Remote Sens.*, vol. 7, no. 5, pp. 1658–1664, May 2014, doi: 10.1109/JSTARS.2013.2273563.

[27] Y. Yang, A. Marshak, S. P. Palm, T. Varnai, and W. J. Wiscombe, "Cloud impact on surface altimetry from a spaceborne 532-nm micropulse photon-counting lidar: System modeling for cloudy and clear atmospheres," *IEEE Trans. Geosci. Remote Sens.*, vol. 49, no. 12, pp. 4910–4919, Dec. 2011, doi: 10.1109/TGRS.2011.2153860.

[28] A. Neuenschwander, E. Guenther, J. C. White, L. Duncanson, and P. Montesano, "Validation of ICESat-2 terrain and canopy heights in boreal forests," *Remote Sens. Environ.*, vol. 251, 2020, Art. no. 112110, doi: 10.1016/j.rse.2020.112110.

[29] S. W. Cooley, J. C. Ryan, and L. C. Smith, "Human alteration of global surface water storage variability," *Nature*, vol. 591, no. 7848, pp. 78–81, 2021, doi: 10.1038/s41586-021-03262-3.

[30] C. Yuan, P. Gong, and Y. Q. Bai, "Performance assessment of ICESat-2 laser altimeter data for water-level measurement over lakes and reservoirs in China," *Remote Sens.*, vol. 12, no. 5, 2020, Art. no. 770, doi: 10.3390/rs12050770.

[31] V. H. Phan, R. Lindenbergh, and M. Menenti, "ICESat derived elevation changes of Tibetan lakes between 2003 and 2009," *Int. J. Appl. Earth Observation Geoinformation*, vol. 17, pp. 12–22, 2012, doi: 10.1016/j.jag.2011.09.015.

[32] G. Zhang, H. Xie, S. Duan, M. Tian, and D. Yi, "Water level variation of Lake Qinghai from satellite and in situ measurements under climate change," *J. Appl. Remote Sens.*, vol. 5, 2011, Art. no. 053532, doi: 10.1117/1.3601363.

[33] T. Chen, C. Song, P. Zhan, and J. Ma, "How many pan-arctic lakes are observed by ICESat-2 in space and time?," *Remote Sens.*, vol. 14, no. 23, 2022, Art. no. 5971, doi: 10.3390/rs14235971.

[34] R. Dubayah et al., "The global ecosystem dynamics investigation: High-resolution laser ranging of the Earth's forests and topography," *Sci. Remote Sens.*, vol. 1, 2020, Art. no. 100002, doi: 10.1016/j.srs.2020.100002.

[35] I. Fayad, N. Baghdadi, J. S. Bailly, F. Frappart, and M. Zribi, "Analysis of gedi elevation data accuracy for inland waterbodies altimetry," *Remote Sens.*, vol. 12, no. 17, 2020, Art. no. 2714, doi: 10.3390/rs12172714.

[36] J. Xiang, H. Li, J. Zhao, X. Cai, and P. Li, "Inland water level measurement from spaceborne laser altimetry: Validation and comparison of three missions over the Great Lakes and lower Mississippi river," *J. Hydrol.*, vol. 597, 2021, Art. no. 126312, doi: 10.1016/j.jhydrol.2021.126312.

[37] I. Fayad, N. Baghdadi, J. S. Bailly, F. Frappart, and N. Pantaleoni Reluy, "Correcting GEDI water level estimates for inland waterbodies using machine learning," *Remote Sens.*, vol. 14, no. 10, 2022, Art. no. 2361, doi: 10.3390/rs14102361.

[38] Y. B. Sulistioadi et al., "Satellite radar altimetry for monitoring small rivers and lakes in Indonesia," *Hydrol. Earth Syst. Sci.*, vol. 19, pp. 341–359. 2015, doi: 10.5194/hess-19-341-2015.

[39] S. Shu et al., "Analysis of Sentinel-3 SAR altimetry waveform retracking algorithms for deriving temporally consistent water levels over ice-covered lakes," *Remote Sens. Environ.*, vol. 239, 2020, Art. no. 111643, doi: 10.1016/j.rse.2020.111643.

[40] Q. Huang, X. Li, P. Han, D. Long, F. Zhao, and A. Hou, "Validation and application of water levels derived from Sentinel-3A for the Brahmaputra River," *Sci. China Technological Sci.*, vol. 62, pp. 1760–1772, 2019, doi: 10.1007/s11431-019-9535-3.

[41] J. Qiu, "China: The third pole," *Nature*, vol. 454, no. 7203, pp. 393–396. 2008, doi: 10.1038/454393a.

[42] X. Kuang and J. J. Jiao, "Review on climate change on the tibetan plateau during the last half century," *J. Geophysical Res., Atmospheres*, vol. 121, no. 8, pp. 3979–4007, 2016, doi: 10.1002/2015JD024728.
[43] F. Yao, J. Wang, C. Wang, and J. F. Crétaux, "Constructing long-term high-frequency time series of global lake and reservoir areas using landsat imagery," *Remote Sens. Environ.*, vol. 232, 2019, Art. no. 111210, doi: 10.1016/j.rse.2019.111210.
[44] F. Xu, G. Zhang, S. Yi, and W. Chen, "Seasonal trends and cycles of lake-level variations over the Tibetan30 Plateau using multi-sensor altimetry data," *J. Hydrol.*, vol. 604, 2022, Art. no. 127251, doi: 10.1016/j.jhydrol.2021.127251.
[45] Z. Zhang, S. Jin, X. Guo, and Y. Bo, "Water level variation in Qinghai Lake from global ecosystem dynamics investigation (GEDI) altimetry data," in *Proc. Photon. Electromagnetics Res. Symp.*, Hangzhou, China, 2021, pp. 2248–2253, doi: 10.1109/PIERS53385.2021.9695004.
[46] T. P. Barnett, J. C. Adam, and D. P. Lettenmaier, "Potential impacts of a warming climate on water availability in snow-dominated regions," *Nature*, vol. 438, pp. 303–309. 2005, doi: 10.1038/nature04141.
[47] C. B. Field et al., "Climate change 2014: Impacts, adaptation, and vulnerability–Part A: Global and sectoral aspects," in *Contribution of Working Group II to The Fifth Assessment Report of The Intergovernmental Panel on Climate Change*. Cambridge, U. K.: Cambridge Univ. Press, , 2014.
[48] R. Ma et al., "A half-century of changes in China's Lakes: Global warming or human influence?," *Geophysical Res. Lett.*, vol. 37, no. 24, 2010, Art. no. L24106, doi: 10.1029/2010GL045514.
[49] I. Fayad, N. Baghdadi, and K. Lahssini, "An assessment of the GEDI lasers' capabilities in detecting canopy tops and their penetration in a densely vegetated, tropical area," *Remote Sens.*, vol. 14, no. 13, 2022, Art. no. 2969, doi: 10.3390/rs14132969.
[50] T. Markus et al., "The ice, cloud, and land elevation satellite-2 (ICESat-2): Science requirements, concept, and implementation," *Remote Sens. Environ.*, vol. 190, pp. 260–273, 2017, doi: 10.1016/j.rse.2016.12.029.
[51] C. E. Parrish, L. A. Magruder, A. L. Neuenschwander, N. Forfinski-Sarkozi, M. Alonzo, and M. Jasinsk, "Validation of ICESat-2 ATLAS bathymetry and analysis of ATLAS's bathymetric mapping performance," *Remote Sens.*, vol. 11, no. 14, 2019, Art. no. 1634, doi: 10.3390/rs11141634.
[52] J. C. Ryan, L. C. Smith, S. W. Cooley, L. H. Pitcher, and T. M. Pavelsky, "Global characterization of inland water reservoirs using ICESat-2 altimetry and climate reanalysis," *Geophys. Res. Lett.*, vol. 47, 2020, Art. no. e2020GL088543, doi: 10.1029/2020GL088543.
[53] S. Luo et al., "Refined estimation of lake water level and storage changes on the Tibetan Plateau from ICESat/ICESat-2," *Catena*, vol. 200, 2021, Art. no. 105177, doi: 10.1016/j.catena.2021.105177.
[54] Z. Zhang, Y. Bo, S. Jin, G. Chen, and Z. Dong, "Dynamic water level changes in Qinghai Lake from integrating refined ICESat-2 and GEDI altimetry data (2018–2021)," *J. Hydrol.*, vol. 617, 2023, Art. no. 129007, doi: 10.1016/j.jhydrol.2022.129007.
[55] W. Han et al., "Water level change of Qinghai Lake from ICESat and ICESat-2 laser altimetry," *Remote Sens.*, vol. 14, no. 24, 2022, Art. no. 6212, doi: 10.3390/rs14246212.
[56] M. Jasinski et al., "Algorithm theoretical basis document (ATBD) for along track inland surface water data, ATL13, release 4," May 1, 2021, NASA, MD, USA, 2020, doi: 10.5067/RNI05Y2CJ9FV.
[57] M. Hofton and J. B. Blair, "Algorithm theoretical basis document (ATBD) for GEDI transmit and receive waveform processing for L1 and L2 products," Dec. 4, 2019, Greenbelt, MD, USA: Goddard Space Flight Center, , 2019, [Online]. Available: https://lpdaac.usgs.gov/documents/581/GEDI_WF_ATBD_v1.0.pdf
[58] S. Nie, C. Wang, G. Li, F. Pan, X. Xi, and S. Luo, "Signal-to-Noise ratio–based quality assessment method for ICESat/GLAS waveform data," *Opt. Eng.*, vol. 53, no. 10, 2014, Art. no. 103104, doi: 10.1117/1.OE.53.10.103104.
[59] G. Zhang et al., "Regional differences of lake evolution across China during 1960s–2015 and its natural and anthropogenic causes," *Remote Sens. Environ.*, vol. 221, pp. 386–404, 2019, doi: 10.1016/j.rse.2018.11.038.
[60] P. Li, H. Li, F. Chen, and X. Cai, "Monitoring long-term lake level variations in middle and lower Yangtze basin over 2002–2017 through integration of multiple satellite altimetry datasets," *Remote Sens.*, vol. 12, no. 9, 2020, Art. no. 1448, doi: 10.3390/rs12091448.
[61] M. Kleinherenbrink, P. G. Ditmar, and R. C. Lindenbergh, "Retracking cryosat data in the SARIn mode and robust lake level extraction," *Remote Sens. Environ.*, vol. 152, pp. 38–50, 2014, doi: 10.1016/j.rse.2014.05.014.
[62] M. J. Kuhn et al., "Candan caret: Classification and regression training," *R Packag. Version 6.0-93*, Aug. 9, 2022, [Online]. Available: http://cran.r-project.org/package=caret
[63] L. Breiman, "Random forests," *Mach. Learn.*, vol. 45, pp. 5–32, 2001, doi: 10.1023/A:1010933404324.
[64] L. Jiang, K. Nielsen, O. B. Andersen, and P. Bauer-Gottwein, "Monitoring recent lake level variations on the Tibetan Plateau using Cryosat-2 sarin mode data," *J. Hydrol.*, vol. 544, pp. 109–124, 2017, doi: 10.1016/j.jhydrol.2016.11.024.
[65] G. Q. Zhang et al., "Lake volume and groundwater storage variations in Tibetan Plateau's endorheic basin," *Geophys. Res. Lett.*, vol. 44, no. 11, pp. 5550–5560, 2017, doi: 10.1002/2017GL073773.
[66] P. Zhan et al., "Recent abnormal hydrologic behavior of Tibetan lakes observed by multi-mission altimeters," *Remote Sens.*, vol. 12, no. 18, 2020, Art. no. 2986, doi: 10.3390/rs12182986.
[67] T. Chen, C. Song, L. Ke, J. Wang, K. Liu, and Q. Wu, "Estimating seasonal water budgets in global lakes by using multi-source remote sensing measurements," *J. Hydrol.*, vol. 593, 2021, Art. no. 125781, doi: 10.1016/j.jhydrol.2020.125781.
[68] M. Halicki and T. Niedzielski, "The accuracy of the Sentinel-3A altimetry over Polish rivers," *J. Hydrol.*, vol. 606, 2022, Art. no. 127355, doi: 10.1016/j.jhydrol.2021.127355.
[69] F. Sun et al., "Changing patterns of lakes on the southern tibetan plateau based on multi-source satellite data," *Remote Sens.*, vol. 12, 2020, Art. no. 3450, doi: 10.3390/rs12203450.
[70] C. Schwatke, D. Dettmering, W. Bosch, and F. Seitz, "DAHITI – an innovative approach for estimating water level time series over inland waters using multi-mission satellite altimetry," *Hydrol. Earth Syst. Sci.*, vol. 19, no. 10, pp. 4345–4364, 2015, doi: 10.5194/hess-19-4345-2015.
[71] F. Xu, G. Zhang, S. Yi, and W. Chen, "Seasonal trends and cycles of lake-level variations over the Tibetan plateau using multi-sensor altimetry data," *J. Hydrol.*, vol. 606, 2022, Art. no. 127251, doi: 10.1016/j.jhydrol.2021.127251.
[72] D. Oesch, J. M. Jaquet, R. Klaus, and P. Schenker, "Multi-scale thermal pattern monitoring of a large lake (Lake Geneva) using a multi-sensor approach," *Int. J. Remote Sens.*, vol. 29, no. 20, pp. 5785–5808, 2008, doi: 10.1080/01431160802132786.

Juan Wu received the B.S. degree in geographical information science from Guizhou Normal University, Guiyang, China, in 2017, and the M.S. degree in cartography and geography information system from Northwest A&F University, Yangling, China, in 2020. She is currently working toward the Ph.D. degree in geography with the School of Geography and Ocean Science, Nanjing University, Nanjing, China.

Her research interests include remote sensing and lake atmosphere interaction.

Chang-Qing Ke received the B.S. degree in geography from Shaanxi Normal University, Xi'an, China, in 1993, the M.S. degree in geography from the Lanzhou Institute of Glaciology and Geocryology, Chinese Academy of Sciences, Lanzhou, China, in 1996, and the Ph.D. degree in geography from the Nanjing Institute of Geography and Limnology, Chinese Academy of Sciences, Nanjing, China, in 1999.

From 1999 to 2002, he was a Postdoctoral Research Fellow with the School of Geography and Ocean Science, Nanjing University, Nanjing, where he has been an Associate professor and a Full Professor in remote sensing since 2002 and 2007, respectively. His research interests include satellite image processing, remote sensing of cryosphere and water resource, and climate change.

Yu Cai received the B.S. degree in geography from Nanjing University, Nanjing, China, in 2016, and the Ph.D. degree in geography from the School of Geography and Ocean Science, Nanjing University, Nanjing, China, in 2021.

She is now an Associate Research Fellow with the School of Geography and Ocean Science, Nanjing University.

Her research interests include remote sensing and lake–atmosphere interaction.

Vahid Nourani received the B.S. and M.S. degrees in civil engineering from University of Tabriz, Tabriz, Iran, in 1998 and 2000, respectively. He then continued his graduate study in civil and environmental engineering in the field of hydrology at Shiraz University, Iran and Tohoku University, Japan, and was graduated in 2005.

He was with the Faculty of Civil Engineering, University of Tabriz as Assistant Professor from 2005 to 2009; as Associate Professor from 2009 to 2014; as a Professor from 2014 and with Department of Civil Engineering, University of Minnesota, USA, at 2011 as a visiting Associate Professor and as an Adjunct Professor with Near East University from 2017. He is currently Editor-in-Chief for Journal of Civil & Env. Eng. (Tabriz Univ.), an Associate Editor for *Journal of Hydrology*, the Vice Dean of Civil Engineering Faculty at Tabriz University and director of Excellence Center in Hydroinformatics. His research interests include rainfall-runoff modeling, Hydroinformatics and computational hydraulics.

Jun Chen received the M.S. degree in geography from Southwest University, Chongqing, China, in 2009, and the Ph.D. degree in geography from the School of Geography and Ocean Science, Nanjing University, Nanjing, China, in 2016.

He is currently an Associate Professor with the Department of Environmental and Energy Engineering, Anhui Jianzhu University, Hefei. He is also a Senior Engineer with the Anhui Engineering and Technology Research Center for Smart City, Hefei. His research interests include satellite image processing, remote sensing of resources and environment.

Zheng Duan received the M.S. degree in cartography and GIS from the Graduate University of Chinese Academy of Sciences, Beijing, China, in 2010 and the Ph.D. degree in remote sensing and hydrological model from Delft University of Technology, Delft, The Netherlands, in 2014.

He was a Scientific Consultant with several institutes including UNESCO-IHE, Delft, The Netherlands. He is currently an Associate Professor with the Department of Physical Geography and Ecosystem Science, Lund University, Sweden. His research interests include integration of remote sensing in hydrological model and water balance studies of lakes and catchments, evapotranspiration, and open water evaporation estimation.